

Myosin light chain kinase (MYLK) coding polymorphisms modulate human lung endothelial cell barrier responses via altered tyrosine phosphorylation, spatial localization, and lamellipodial protrusions

Ting Wang^{1,*}, Mary E. Brown^{2,*}, Gabriel T. Kelly¹ , Sara M. Camp¹, Joseph B. Mascarenhas¹, Xiaoguang Sun¹, Steven M. Dudek² and Joe G.N. Garcia¹

¹Department of Medicine, University of Arizona Health Sciences, Tucson, AZ, USA; ²Department of Medicine, University of Illinois at Chicago, Chicago, IL, USA

Abstract

Sphingosine 1-phosphate (SIP) is a potent bioactive endogenous lipid that signals a rearrangement of the actin cytoskeleton via the regulation of non-muscle myosin light chain kinase isoform (nmMLCK). SIP induces critical nmMLCK Y⁴⁶⁴ and Y⁴⁷¹ phosphorylation resulting in translocation of nmMLCK to the periphery where spatially-directed increases in myosin light chain (MLC) phosphorylation and tension result in lamellipodia protrusion, increased cell-cell adhesion, and enhanced vascular barrier integrity. *MYLK*, the gene encoding nmMLCK, is a known candidate gene in lung inflammatory diseases, with coding genetic variants (Pro21His, Ser147Pro, Val261Ala) that confer risk for inflammatory lung injury and influence disease severity. The functional mechanisms by which these *MYLK* coding single nucleotide polymorphisms (SNPs) affect biologic processes to increase disease risk and severity remain elusive. In the current study, we utilized quantifiable cell immunofluorescence assays to determine the influence of *MYLK* coding SNPs on SIP-mediated nmMLCK phosphorylation and translocation to the human lung endothelial cell (EC) periphery. These disease-associated *MYLK* variants result in reduced levels of SIP-induced Y⁴⁶⁴ phosphorylation, a key site for nmMLCK enzymatic regulation and activation. Reduced Y⁴⁶⁴ phosphorylation resulted in attenuated nmMLCK protein translocation to the cell periphery. We further conducted EC kymographic assays which confirmed that lamellipodial protrusion in response to SIP challenge was retarded by expression of a *MYLK* transgene harboring the three *MYLK* coding SNPs. These data suggest that ARDS/severe asthma-associated *MYLK* SNPs functionally influence vascular barrier-regulatory cytoskeletal responses via direct alterations in the levels of nmMLCK tyrosine phosphorylation, spatial localization, and lamellipodial protrusions.

Keywords

sphingosine 1-phosphate, SIP, nmMLCK, SNP

Date received: 17 July 2017; accepted: 19 February 2018

Pulmonary Circulation 2018; 8(2) 1–7

DOI: 10.1177/2045894018764171

Introduction

The essential role of the non-muscle myosin light chain kinase isoform or nmMLCK¹ in the complex regulation of endothelial cell cytoskeleton rearrangement, especially during disruption and restoration of vascular integrity, has been well defined.^{2–8} Acute and chronic cardiovascular diseases, including acute lung injury (ALI) and its more severe form acute respiratory distress syndrome (ARDS),⁹ have obvious uncontrolled pulmonary vascular hyper-permeability

which has been determined to be the major cause of pulmonary alveolar edema.¹⁰ The major translational product of the *MYLK* gene in endothelium is the non-muscle isoform of MLCK (nmMLCK, 210 kd). Both nmMLCK and the

*Equal contributors.

Corresponding author:

Joe G.N. Garcia, University of Arizona Health Sciences, 1295 N. Martin Avenue, PO Box 210202, Tucson, AZ 85721-0202, USA.

Email: skipgarcia@email.arizona.edu



Creative Commons Non Commercial CC-BY-NC: This article is distributed under the terms of the Creative Commons Attribution-NonCommercial 4.0 License (<http://www.creativecommons.org/licenses/by-nc/4.0/>)

which permits non-commercial use, reproduction and distribution of the work without further permission provided the original work is attributed as specified on the SAGE and Open Access pages (<https://us.sagepub.com/en-us/nam/open-access-at-sage>).

© The Author(s) 2018.

Reprints and permissions:
sagepub.co.uk/journalsPermissions.nav
journals.sagepub.com/home/pul



smooth muscle isoform of MLCK (smMLCK, 135 kd)¹ share identical c-terminal domains including the calmodulin (CaM)-binding domain and catalytic domain.³ nmMLCK, however, carries an additional, highly unique, N-terminus that is modulated via post-translational modifications.^{5,7} Interestingly, during the development phase of ALI/ARDS, edemagenic agonists—such as thrombin, TNF α , or LPS—induce phosphorylation (Y⁴⁶⁴ and Y⁴⁷¹) via p60-c-Src, leading to activation of nmMLCK, increases in myosin light chain (MLC) phosphorylation and accelerated formation of intracellular polymerized actin filaments or stress fibers.^{5,11} These events cause cortical filament loss, profound stress fiber formation, and centrally distributed contractile tension that directly leads to vascular hyper-permeability and fluid leakage. In contrast, during barrier recovery or in response to endogenous EC barrier enhancers, such as sphingosine 1-phosphate (S1P) or hepatocyte growth factor (HGF),^{12,13} nmMLCK again undergoes c-Abl-catalyzed phosphorylation at the same sites (Y⁴⁶⁴ and Y⁴⁷¹)⁷ resulting in increases in EC cortically distributed tension,^{14–17} lamellipodial protrusions, increased cell-cell adhesion, barrier enhancement, and gap closure.⁷ C-Abl is a Src kinase family member, that binds, phosphorylates, and transports nmMLCK to the cell periphery.⁷ This underscores the complexity and duality of nmMLCK's role in vascular barrier regulation in a highly agonist-dependent manner linked to dynamic phasic barrier regulation (inflammation development vs. inflammation resolution).

These important functions of nmMLCK have made *MYLK* a very compelling candidate gene for vasculature-driven diseases. Earlier interrogation of *MYLK* as a candidate gene in inflammatory lung disease involving pulmonary vascular hyper-permeability demonstrated *MYLK* single nucleotide polymorphisms (SNPs) to confer risk and severity in ALI/ARDS^{18–20} and in severe asthma.^{21–24} Three *MYLK* single nucleotide polymorphisms (SNPs) resulting in variants Pro21His, Ser147Pro, and Val261Ala, each residing in the nmMLCK N-terminus, in high linkage disequilibrium, confer significant ARDS risk¹⁸ and Pro147Ser was a risk variant for severe asthma.²² Each of these SNPs were uncommon in non-Hispanic Caucasians but exhibited high minor allelic frequencies in individuals of African descent (AD), a racial group at significantly greater risk and higher mortality in sepsis, ARDS, and severe asthma.²⁵

We recently reported the SNP resulting in Ser147Pro to influence *MYLK* transcription and secondary mRNA structure.²⁴ thereby leading to elevated expression of nmMLCK. However, the mechanisms by which *MYLK* coding SNPs impact nmMLCK cellular function, cellular trafficking, or phosphorylation to alter cellular physiologic responses are unknown. In this study, we assessed the influence of these three genetically linked *MYLK* coding SNPs (resulting in variants Pro21His, Ser147Pro, Val261Ala), as well as a single inflammatory lung disease associated SNP (resulting in Ser147Pro) on S1P-mediated nmMLCK localization, phosphorylation (Y⁴⁶⁴), and lamellipodia dynamics.

Methods

Reagents

Chemicals and biochemicals, including S1P, were obtained from Sigma (St. Louis, MO, USA) unless otherwise specified. Paraformaldehyde was purchased from Fisher Scientific (Fair Lawn, NJ, USA). Fluorescent dye-labeled reagents and Prolong Gold with DAPI were obtained from Molecular Probes (Eugene, OR, USA). Human lung microvascular endothelial cell (EC) and culture reagents were purchased from Lonza (Walkersville, MD, USA). Phosphotyrosine 464 (Y⁴⁶⁴) nmMLCK antibody was obtained from Ameritech (Houston, TX, USA). Secondary antibodies were purchased from Cell Signaling (Danvers, MA, USA). The nmMLCK constructs (wild type or mutated) were generated in our lab and have been reported previously.²⁶ Transfection reagent X-fect was purchased from Clontech/Takara (Mountain View, CA, USA).

Human EC culture

Human lung microvascular ECs were cultured with Lonza recommended protocols and reagents. In brief, ECs were cultured in complete growth medium consisting of Endothelial Growth Medium 2 (EGM2) and incubated at 37°C in a humidified atmosphere of 5% CO₂ and 95% air as we have previously described.²⁶ ECs were utilized at passages 6–8.

Immunofluorescence

ECs transfected with one of the three EGFP-nmMLCK constructs (wild type [WT], Ser147Pro, or 3SNP-Pro21His, Ser147Pro, Val261Ala) were added to a 12-well plate containing a gelatin-coated 18-mm glass coverslip in each well and allowed to recover in complete medium for 6–8 h. Transfected EC were stimulated at 37°C with 1 μ M S1P (2–10 min). Coverslips were washed with Tris-buffered saline (TBS) and transferred to wells containing 4% paraformaldehyde in TBS. Following fixation for 20 min at room temperature, ECs were washed and unreacted aldehyde groups were quenched in 50 mM NH₄Cl/TBS followed by three washes in TBS (5 min each). Slides were then incubated in 0.1% Triton X-100/TBS for 15 min at room temperature for cell permeabilization. The cells then were incubated with blocking buffer (5% BSA in TBS) for 30 min, and primary antibody (phosphotyrosine 464 (Y⁴⁶⁴) nmMLCK antibody, 1:200 dilution in blocking buffer) for 1 h. Following three washes in blocking buffer, cells were incubated in secondary antibody (1:200 dilution in blocking buffer) for 30 min. Following three washes in blocking buffer, F-actin was stained by incubating the cells in 5 units/mL phalloidin-rhodamine/blocking solution for 30 min in the dark. Finally, ECs were washed three times for 5 min each in blocking solution, then mounted in 10 μ L of Prolong Gold with DAPI and preserved in the dark. ECs were imaged on

a Leica TCS SP5 AOTF laser-scanning confocal microscopy system scanning at 400 Hz. Twelve-bit 512×512 images were acquired sequentially (with a line average setting of 16) with Leica LAS AF software and detected with a photomultiplier tube. All post-acquisition image processing was performed with the ImageJ software bundle (<http://rsb.info.nih.gov/ij/>).

Quantification of lamellipodia localization

ECs transfected with EGFP-nmMLCK constructs (one of the three types) were challenged with S1P. Lamellipodia localization of nmMLCK was quantified with an established method.²⁶ The EGFP-nmMLCK images were background-subtracted and a region of interest (ROI) was drawn around individual cells. All areas outside the cell were cleared in order to best visualize the leading edges of lamellipodia and the fluorescence intensity within an entire cell was summed. The percentage of EGFP-nmMLCK in lamellipodia was calculated from the ratio of the summed fluorescence intensities within selected lamellipodia to the summed fluorescence intensity of the entire cell.

Live EC imaging

We utilized an established method for live cell imaging and kymograph analysis.^{8,26} Briefly, EC grown on coverslips were loaded into a recording chamber (ALA Scientific Instruments, Westbury, NY, USA) in culture media at 37°C. Images were acquired by a Zeiss 710 laser scanning confocal microscope (every 6 s) and cells were observed under basal conditions and 10 min post administration of 1 μ M S1P. Images were analyzed using ImageJ and kymographic analysis was performed using the Multiple Kymograph Plugin to assess membrane dynamics as we have described previously.^{8,26}

Statistical analysis

Data are presented as mean \pm standard error. Statistical significance ($P < 0.05$) was determined with two-way ANOVA (for more than two groups) or with an unpaired Student's t-test (for only two groups).

Results

MYLK SNPs influence S1P-induced nmMLCK1 phosphorylation and translocation to the EC periphery

S1P induces activation of c-Abl kinase,⁷ resulting in nmMLCK phosphorylation and nmMLCK-cortactin colocalization within lamellipodia,⁶ leading to EC lamellipodia protrusion and paracellular gap closure, which are essential for vascular barrier maintenance and restoration during the inflammation resolution phase. We first examined the influence of genetic variants on these events. The plasmids EGFP-nmMLCK1 wild type (WT-nmMLCK1), EGFP-nmMLCK1-S147P (S147P-nmMLCK1), and EGFP-

nmMLCK1-P21H/S147P/V261A (3SNP-nmMLCK1) were each ectopically expressed in human lung microvascular ECs (24 h) and stimulated with S1P (1 μ M, 2 min or 5 min), fixed, and analyzed via immunofluorescence with a nmMLCK1 phospho-Y⁴⁶⁴-specific antibody (Fig. 1) and phalloidin staining for polymerized actin. S1P challenge robustly induced enrichment of polymerized actin in the cell periphery and translocation of nmMLCK1 to the cell periphery with F-actin co-localization.

Figure 2 depicts that levels of S1P-stimulated nmMLCK1 phosphorylation at Y⁴⁶⁴, known to increase nmMLCK enzymatic activation,^{5,7} are reduced in both mutant nmMLCK1 proteins when compared to WT-nmMLCK1. Modest reductions in phospho-Y⁴⁶⁴ mean fluorescence intensities were noted in both variant nmMLCK1 proteins at each S1P treatment time point as well as in unstimulated controls when compared to respective wild types. The largest differences in Y⁴⁶⁴ phosphorylation occurred at 2 min of S1P stimulation, with average fluorescence intensity/ μm^2 decreasing by 20% for S147P-nmMLCK1 and by 40% for 3SNP-nmMLCK1 when compared to WT-nmMLCK1. At 5 min of S1P stimulation, Y⁴⁶⁴ phosphorylation in S147P and the 3SNP variant were reduced 14% and 32%, respectively, compared to WT-nmMLCK1.

We next evaluated whether reductions in nmMLCK1 Y⁴⁶⁴ phosphorylation altered translocation of nmMLCK1 to the cell periphery. Quantification of S1P (1 μ M, 2–10 min)-induced nmMLCK1 phosphorylation and translocation to EC lamellipodia (Fig. 3) revealed both mutant nmMLCK1 proteins (S147P or 3SNP) to significantly reduce translocation of nmMLCK1 to lamellipodia compared to the WT-nmMLCK1. In addition, the 3SNP-nmMLCK1 protein exhibited reduced lamellipodia translocation when compared to S147P-nmMLCK1. A similar pattern of localized phospho-MLC was also observed post S1P challenge in WT-nmMLCK1 or 3SNP-nmMLCK1 transfected ECs, where the more phosphorylated MLC was located in lamellipodia in WT-nmMLCK1 transfected cells than 3SNP-nmMLCK1 transfected cells (Supplementary Figure S1).

These results indicate that *MYLK* SNPs (S147P or 3SNP) associated with risk and severity of inflammatory lung disease suppress S1P-mediated nmMLCK1 phosphorylation and translocation to the cell periphery and to lamellipodia, events that are critical to vascular barrier restoration and recovery.²⁷

MYLK SNPs modulate S1P-stimulated kymographic dynamics in lamellipodia protrusions in human endothelium

We next utilized live cell imaging to confirm the influence of *MYLK* SNPs on kymographic/lamellipodial dynamics. Dynamic measurements of lamellipodia protrusion suggested that S1P-mediated lamellipodia protrusion is slowed in ECs transfected with SNP-containing nmMLCK1, compared to transfection with a WT-nmMLCK1 transgene, as measured by prolonged process (increased time to reach

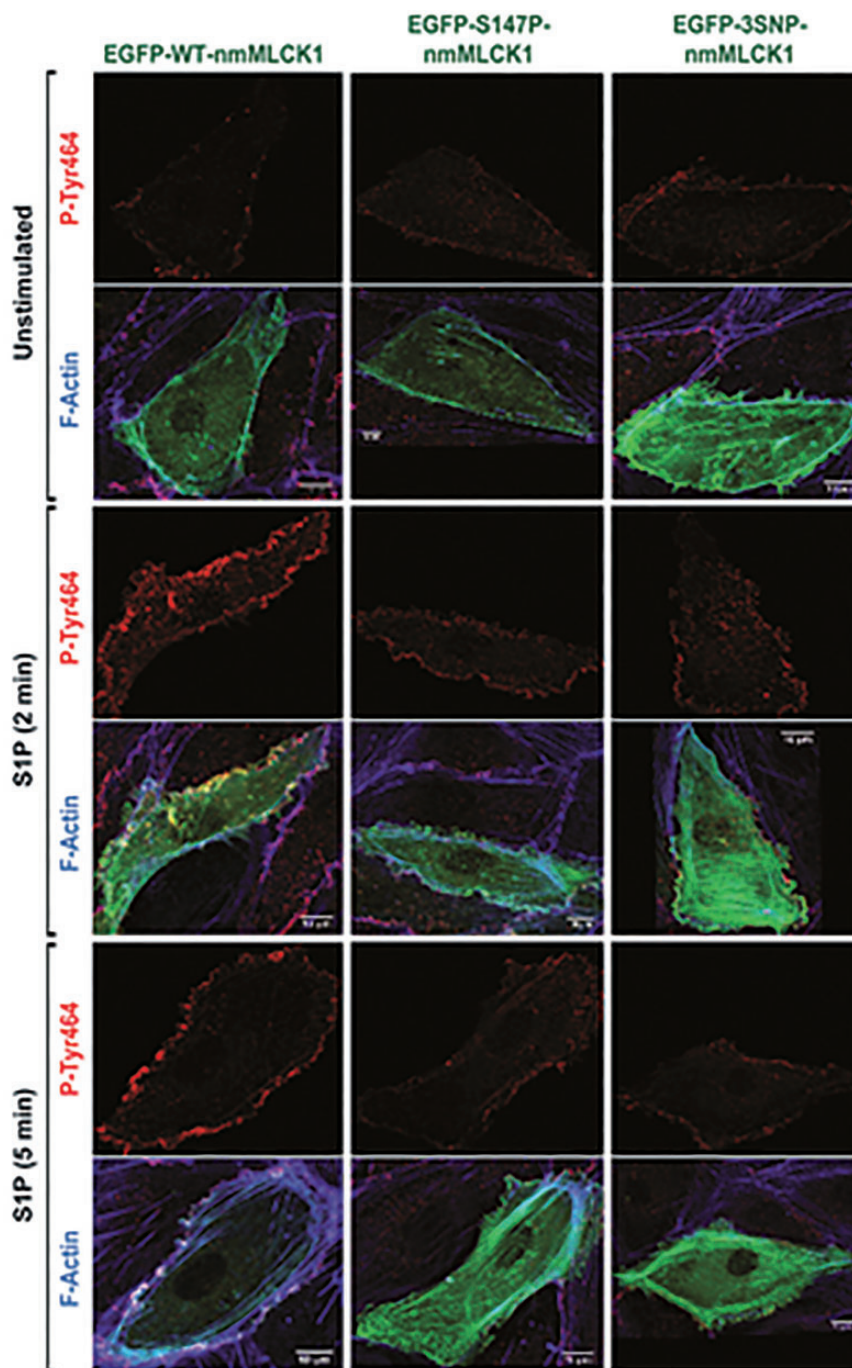


Fig. 1. nmMLCK1 Y⁴⁶⁴ phosphorylation and cellular localization upon S1P challenge. Human pulmonary microvascular ECs were transfected with EGFP-nmMLCK1 constructs with WT, S147P, or 3SNP. Then ECs were challenged with S1P (1 μ M) for 2 or 5 min. Immunofluorescence assays were performed to visualize nmMLCK Y⁴⁶⁴ phosphorylation (red), F-actin (blue), and transfected EGFP-nmMLCK1 (green). These representative images were selected from > 5 independent assays.

maximum distance), and by shorter distance of protrusion (Table 1). These kymographic findings suggest that both S147P- or 3SNP-containing nmMLCK proteins exhibit an impairment in lamellipodia formation dynamics, and thus reduced capacity for rapid EC barrier restoration elicited by S1P challenge. There were no significant differences noted between S147P- and 3SNP-nmMLCK1 mutant

proteins in kymographic indices involved in lamellipodia protrusion.

Discussion

S1P-mediated nmMLCK activation by Y⁴⁶⁴ phosphorylation and subsequent localization in lamellipodia are considered

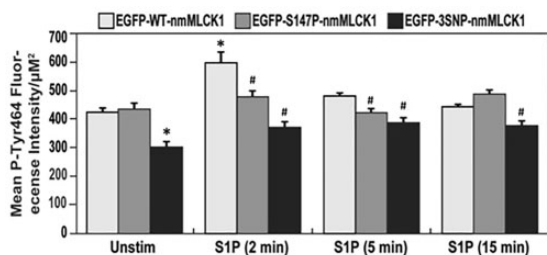


Fig. 2. Effects of genetic variants on nmMLCK1 Y⁴⁶⁴ phosphorylation post SIP challenge. Human pulmonary microvascular ECs were transfected with EGFP-nmMLCK1 constructs with WT, S147P, or 3SNP. Then ECs were challenged with SIP (1 µM) for 2–15 min. Immunofluorescence assays were performed to visualize nmMLCK1 Y⁴⁶⁴ phosphorylation. Relative nmMLCK1 Y⁴⁶⁴ phosphorylation levels in ECs were quantified. n = 30. *P < 0.05 compared to unstimulated WT EGFP-nmMLCK1 (the first white bar). #P < 0.05 compared to WT EGFP-nmMLCK1 group at the same time point of SIP challenge (the white bar of each time point).

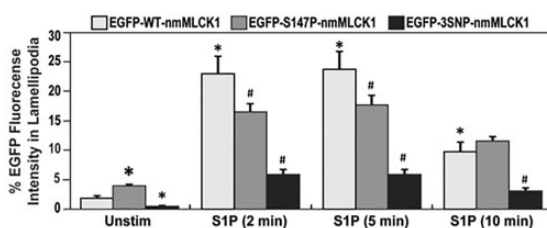


Fig. 3. Effects of genetic variants on nmMLCK1 enrichment in lamellipodia post SIP challenge. Human pulmonary microvascular ECs were transfected with EGFP-nmMLCK1 constructs with WT, S147P, or 3SNP. Then ECs were challenged with SIP (1 µM) for 2–10 min. EGFP levels in lamellipodia were quantified relative to whole cell EGFP levels. n = 30. *P < 0.05 compared to unstimulated WT EGFP-nmMLCK1 (the first white bar). #P < 0.05 compared to WT EGFP-nmMLCK1 group at the same time point of SIP challenge.

key signaling events in pulmonary EC barrier restoration following inflammatory lung injury and vascular hyperpermeability.⁷ We previously reported via live cell imaging that nmMLCK co-localizes with cortactin during membrane ruffling and rapid translocation to lamellipodia after SIP challenge²⁶ in concert with c-Abl-mediated nmMLCK and cortactin phosphorylation⁷ resulting in increases in MLC phosphorylation in lamellipodia.²⁶ These events temporally coincide exactly with the rise in trans-EC electrical resistance (TER), a reflection of increasing EC barrier integrity, and increases in elastic modulus, a reflection of intracellular tension at the cell periphery (via atomic force microscopy or AFM)⁷ promoting EC barrier integrity.^{14–17}

We explored the functionality of three *MYLK* SNPs unique to nmMLCK (resulting in variants Pro21His, Ser147Pro, Val261Ala), previously determined to confer increased ARDS and severe asthma risk in individuals of African descent (AD), consistent with the known health disparity that exists for this population in both ARDS and

severe asthma.²⁸ ARDS and asthma have an unacceptable worldwide morbidity and mortality,²⁹ particularly in population of AD who exhibit four times the asthma prevalence and asthma mortality compared to Caucasians.³⁰ The molecular determinants that underlie ARDS and asthma development are unknown with identification of novel genetic variants and targets needed. *MYLK* is one of these genes with high minor allele frequencies in AD patients of ARDS or asthma compared to Caucasian patients.^{18–20,22} Clearly, the identification of the functional effects of these SNPs will increase understanding of the high mortalities of AD patients with these diseases and assist the design of more effective population-selective therapies.

We sought to link *MYLK* SNP functionality to the well-recognized key pathobiological process of vascular barrier dysregulation. We observed that either the inflammatory disease-associated single SNP (Ser147Pro) or the 3SNP containing nmMLCK exhibited reduced nmMLCK1 phosphorylation (Y⁴⁶⁴) and nmMLCK1 translocation to lamellipodia compared with WT-nmMLCK1. We confirmed these findings via live cell imaging to assess kymographic/lamellipodial dynamics and observed significantly slower protrusion/retraction rates and distances with the inflammatory disease-associated SNPs in nmMLCK1. These studies provide support for ARDS SNP functionality in lamellipodial dynamics and paracellular gap closure. These results are consistent with nmMLCK1 participation in actin polymerization and lamellipodia force development utilizing atomic force microscopy (AFM) to measure EC cytoskeletal tension at specific cellular sites as we previously described.⁷ Human lung ECs, transfected with WT-nmMLCK1 or nmMLCK1 harboring the triple SNPs (P21H/S147P/V261A), were dynamically analyzed by AFM screening of nuclear, cytosolic, and lamellipodial cell regions.^{7,14–16} Increased elastic modulus was localized to cytosolic stress fibers, a reflection of intracellular force and tension generation, in WT-nmMLCK1 transfected ECs after thrombin challenge, whereas a cortical distribution was observed after SIP challenge.²⁶ The triple SNP nmMLCK1 mutant protein exhibited greater thrombin-mediated tension/force generation in stress fibers but a striking reduction in force generation in lamellipodia after SIP treatment (data not shown). These results together confirm the influence of ARDS-associated coding SNPs on nmMLCK1 function and activation in a SIP-driven signaling cascade, one of the most robust (to our knowledge) endogenous signaling pathway leading to EC paracellular gap closure and barrier restoration.

While our current study identifies that these inflammatory disease-associated SNPs alter the normal translocation and Y⁴⁶⁴ phosphorylation responses of nmMLCK1 to SIP challenge, these barrier-restoring events are not the sole functional influences of these SNPs on nmMLCK1. In a previous study with a different computational biology approach, we identified that S147P (rs9840993) exerts a significant impact on *MYLK* mRNA secondary structure.²⁴

Table 1. Protrusion kymographic dynamics in response to SIP in ECs transfected with nmMLCK1.

| nmMLCK1 proteins | WT-nmMLCK1 | S147P-nmMLCK1 | 3SNP-nmMLCK1 |
|--------------------------|-------------|---------------|--------------|
| Speed (nm/s) | 67.2 ± 5.80 | 35.4 ± 5.55* | 34.2 ± 3.45* |
| Distance (nm) | 2641 ± 183 | 1747 ± 309.4* | 2115 ± 161* |
| Time to max distance (s) | 42.4 ± 4.98 | 59.6 ± 13.7* | 70.0 ± 8.44* |

n = 20–30.

*P < 0.05 compared to WT-nmMLCK1 transfected cells.

This structural alteration leads to persistent changes on mRNA stability and translation efficiency (not dependent on any agonist).²⁴ We also examined the structural impact of these SNPs on nmMLCK N-terminus using combined approaches including nuclear magnetic resonance (NMR) and molecular modeling.³¹ Both NMR analysis and molecular modeling indicated these three SNPs localize in the loops that connect the immunoglobulin-like domains of nmMLCK and exert minimal structural impact on the nmMLCK N-terminus.³¹ In addition, it is suggested that S147P might influence protein–protein interaction motifs located in nmMLCK, which interfere with binding to the scaffold protein, 14-3-3.³¹ Despite this speculation, the consequences of these potential structural impacts are not known, consistent with the complex functionality of these inflammatory disease-associated SNPs in nmMLCK.

ECs express two major splice variants of nmMLCK by alternative splicing (nmMLCK1 and nmMLCK2). nmMLCK1 differs from nmMLCK2 only by the inclusion of exon 11 (where Y⁴⁶⁴ resides), allowing for more robust nmMLCK1 regulation by tyrosine kinases (e.g. c-Src or c-Abl) compared to nmMLCK2 which has exon 11 deleted via alternative splicing.^{1,32} We recently demonstrated that ARDS-related stimuli drive alternative splicing that favors greater expression of nmMLCK2, and thus less regulation by barrier-restoring stimuli, such as SIP and HGF, and consequently persistent gap formation.³²

We also examined the effects of SIP-mediated nmMLCK2 protrusion in lamellipodia dynamics, serving as a control to the effects on nmMLCK1, since nmMLCK2 does not contain Y⁴⁶⁴, the key regulatory phosphorylation site in nmMLCK1. Compared to nmMLCK1, the splice variant nmMLCK2 exhibited reduced lamellipodia protrusion speed and prolonged protrusion processes (i.e. longer time to reach maximum distance) (Supplementary Table S1, Supplementary Figure S2). Unlike nmMLCK1, S147P- and 3SNP-containing mutant proteins do not consistently alter protrusion speed in nmMLCK2. Kymography revealed lamellipodia protrusion of S147P-nmMLCK2 overexpression cells is more rapid than that of WT-nmMLCK2, whereas 3SNP-nmMLCK2 overexpression cells exhibit comparable speeds (Supplementary Table S1, Supplementary Figure S2). Interestingly, while both variant-containing nmMLCK1 proteins exhibited reduced protrusion compared to WT-nmMLCK1 (Table 1), these variants exerted differential effects in nmMLCK2. These data suggest the likelihood

that a different molecular mechanism activated by SIP may regulate nmMLCK2, possibly leading to a differential cell response.

Interestingly, it is noticeable that SIP-mediated nmMLCK phosphorylation peaks around 2–5 min, while Abl kinase activity, which is responsible for the Y464 phosphorylation upon SIP challenge, is indeed increased (0–15 min) time-dependently.⁷ These inconsistent results suggest the involvement of activated nmMLCK phosphatase by SIP, as SIP is known to activate specific protein phosphatases.³³ This possible mechanism serves as the basis of dynamic and precise control of EC barrier by SIP via nmMLCK regulation.

Taken together, our study has confirmed that these three inflammatory disease-associated MYLK SNPs directly impact nmMLCK localization and phosphorylation in response to SIP, and suggests that these genetic variants exert functional impacts on EC barrier regulation to impose an adverse effect in inflammatory disease clinical outcomes.

Conflict of interest

The author(s) declare that there is no conflict of interest.

Funding

These studies were supported by National Institutes of Health grants P01-HL126609 (JGNG), R01-HL125615 (JGNG), R01-HL91899 (JGNG and TW), P01-HL134610 (JGNG and TW).

ORCID iD

Gabriel T. Kelly  <http://orcid.org/0000-0003-3549-5229>

References

- Lazar V and Garcia JG. A single human myosin light chain kinase gene (MLCK; MYLK). *Genomics* 1999; 57(2): 256–267.
- Garcia JG, Davis HW and Patterson CE. Regulation of endothelial cell gap formation and barrier dysfunction: role of myosin light chain phosphorylation. *J Cell Physiol* 1995; 163(3): 510–522.
- Davis HW, Crimmins DL, Thoma RS, et al. Phosphorylation of calmodulin in the first calcium-binding pocket by myosin light chain kinase. *Arch Biochem Biophys* 1996; 332(1): 101–109.
- Garcia JG, Verin AD, Schaphorst K, et al. Regulation of endothelial cell myosin light chain kinase by Rho, cortactin, and p60(src). *Am J Physiol* 1999; 276(6 Pt 1): L989–998.
- Birukov KG, Csontos C, Marzilli L, et al. Differential regulation of alternatively spliced endothelial cell myosin light chain

- kinase isoforms by p60(Src). *J Biol Chem* 2001; 276(11): 8567–8573.
6. Dudek SM, Birukov KG, Zhan X, et al. Novel interaction of cortactin with endothelial cell myosin light chain kinase. *Biochem Biophys Res Commun* 2002; 298(4): 511–519.
 7. Dudek SM, Chiang ET, Camp SM, et al. Abl tyrosine kinase phosphorylates nonmuscle Myosin light chain kinase to regulate endothelial barrier function. *Mol Biol Cell* 2010; 21(22): 4042–4056.
 8. Belvitch P, Adyshev D, Elangovan VR, et al. Proline-rich region of non-muscle myosin light chain kinase modulates kinase activity and endothelial cytoskeletal dynamics. *Microvasc Res* 2014; 95: 94–102.
 9. Kollef MH and Schuster DP. The acute respiratory distress syndrome. *N Engl J Med* 1995; 332(1): 27–37.
 10. Dudek SM and Garcia JG. Cytoskeletal regulation of pulmonary vascular permeability. *J Appl Physiol (1985)* 2001; 91(4): 1487–1500.
 11. Petrache I, Birukov K, Zaiman AL, et al. Caspase-dependent cleavage of myosin light chain kinase (MLCK) is involved in TNF-alpha-mediated bovine pulmonary endothelial cell apoptosis. *Faseb J* 2003; 17(3): 407–416.
 12. Dudek SM, Jacobson JR, Chiang ET, et al. Pulmonary endothelial cell barrier enhancement by sphingosine 1-phosphate: roles for cortactin and myosin light chain kinase. *J Biol Chem* 2004; 279(23): 24692–24700.
 13. Liu F, Schaphorst KL, Verin AD, et al. Hepatocyte growth factor enhances endothelial cell barrier function and cortical cytoskeletal rearrangement: potential role of glycogen synthase kinase-3beta. *Faseb J* 2002; 16(9): 950–962.
 14. Birukova AA, Arce FT, Moldobaeva N, et al. Endothelial permeability is controlled by spatially defined cytoskeletal mechanics: atomic force microscopy force mapping of pulmonary endothelial monolayer. *Nanomedicine* 2009; 5(1): 30–41.
 15. Arce FT, Meckes B, Camp SM, et al. Heterogeneous elastic response of human lung microvascular endothelial cells to barrier modulating stimuli. *Nanomedicine* 2013; 9(7): 875–884.
 16. Wang X, Bleher R, Brown ME, et al. Nano-biomechanical study of spatio-temporal cytoskeleton rearrangements that determine subcellular mechanical properties and endothelial permeability. *Sci Rep* 2015; 5: 11097.
 17. Viswanathan P, Ephstein Y, Garcia JG, et al. Differential elastic responses to barrier-altering agonists in two types of human lung endothelium. *Biochem Biophys Res Commun* 2016; 478(2): 599–605.
 18. Christie JD, Ma SF, Aplenc R, et al. Variation in the myosin light chain kinase gene is associated with development of acute lung injury after major trauma. *Crit Care Med* 2008; 36(10): 2794–2800.
 19. Gao L, Grant A, Halder I, et al. Novel polymorphisms in the myosin light chain kinase gene confer risk for acute lung injury. *Am J Respir Cell Mol Biol* 2006; 34(4): 487–495.
 20. Gao L, Grant AV, Rafaels N, et al. Polymorphisms in the myosin light chain kinase gene that confer risk of severe sepsis are associated with a lower risk of asthma. *J Allergy Clin Immunol* 2007; 119(5): 1111–1118.
 21. Acosta-Herrera M, Pino-Yanes M, Ma SF, et al. Fine mapping of the myosin light chain kinase (MYLK) gene replicates the association with asthma in populations of Spanish descent. *J Allergy Clin Immunol* 2015; 136(4): 1116–1118.
 22. Flores C, Ma SF, Maresco K, et al. A variant of the myosin light chain kinase gene is associated with severe asthma in African Americans. *Genet Epidemiol* 2007; 31(4): 296–305.
 23. Wang T, Moreno-Vinasco L, Ma SF, et al. Nonmuscle myosin light chain kinase regulates murine asthmatic inflammation. *Am J Respir Cell Mol Biol* 2014; 50(6): 1129–1135.
 24. Wang T, Zhou T, Saadat L, et al. A MYLK variant regulates asthmatic inflammation via alterations in mRNA secondary structure. *Eur J Hum Genet* 2015; 23(6): 874–876.
 25. Moss M and Mannino DM. Race and gender differences in acute respiratory distress syndrome deaths in the United States: an analysis of multiple-cause mortality data (1979–1996). *Crit Care Med* 2002; 30(8): 1679–1685.
 26. Brown M, Adyshev D, Bindokas V, et al. Quantitative distribution and colocalization of non-muscle myosin light chain kinase isoforms and cortactin in human lung endothelium. *Microvasc Res* 2010; 80(1): 75–88.
 27. Garcia JG, Liu F, Verin AD, et al. Sphingosine 1-phosphate promotes endothelial cell barrier integrity by Edg-dependent cytoskeletal rearrangement. *J Clin Invest* 2001; 108(5): 689–701.
 28. Garcia JG and Sznajder JI. Healthcare disparities in patients with acute respiratory distress syndrome. Toward equity. *Am J Respir Crit Care Med* 2013; 188(6): 631–632.
 29. Hughes E, Kilmer G, Li Y, et al. Surveillance for certain health behaviors among states and selected local areas - United States, 2008. *MMWR Surveill Summ* 2010; 59(10): 1–221.
 30. Rosser FJ, Forno E, Cooper PJ, et al. Asthma in hispanics. An 8-year update. *Am J Respir Crit Care Med* 2014; 189(11): 1316–1327.
 31. Shen K, Ramirez B, Mapes B, et al. Structure-function analysis of the non-muscle myosin light chain kinase (nmMLCK) isoform by NMR spectroscopy and molecular modeling: influence of MYLK variants. *PLoS One* 2015; 10(6): e0130515.
 32. Mascarenhas JB, Tchourbanov AY, Fan H, et al. Mechanical stress and single nucleotide variants regulate alternative splicing of the MYLK gene. *Am J Respir Cell Mol Biol* 2017; 56(1): 29–37.
 33. Che W, Manetsch M, Quante T, et al. Sphingosine 1-phosphate induces MKP-1 expression via p38 MAPK- and CREB-mediated pathways in airway smooth muscle cells. *Biochim Biophys Acta* 2012; 1823(10): 1658–1665.